



**HAL**  
open science

## Modified Vaccinia Virus Ankara Vector Induces Specific Cellular and Humoral Responses in the Female Reproductive Tract, the Main HIV Portal of Entry

Romain Marlin, Marie-Thérèse Nugeyre, Nicolas Tchitchek, Matteo Parenti, Hakim Hocini, Fahd Benjelloun, Claude Cannou, Nathalie Dereuddre-Bosquet, Yves Lévy, Françoise Barré-Sinoussi, et al.

### ► To cite this version:

Romain Marlin, Marie-Thérèse Nugeyre, Nicolas Tchitchek, Matteo Parenti, Hakim Hocini, et al.. Modified Vaccinia Virus Ankara Vector Induces Specific Cellular and Humoral Responses in the Female Reproductive Tract, the Main HIV Portal of Entry. *Journal of Immunology*, 2017, 199 (5), pp.1923 - 1932. 10.4049/jimmunol.1700320 . pasteur-01597708

**HAL Id: pasteur-01597708**

**<https://pasteur.hal.science/pasteur-01597708>**

Submitted on 28 Sep 2017

**HAL** is a multi-disciplinary open access archive for the deposit and dissemination of scientific research documents, whether they are published or not. The documents may come from teaching and research institutions in France or abroad, or from public or private research centers.

L'archive ouverte pluridisciplinaire **HAL**, est destinée au dépôt et à la diffusion de documents scientifiques de niveau recherche, publiés ou non, émanant des établissements d'enseignement et de recherche français ou étrangers, des laboratoires publics ou privés.



Distributed under a Creative Commons Attribution - NonCommercial - ShareAlike 4.0 International License

1 **Title**

2 **Modified Vaccinia virus Ankara vector induces specific cellular**  
3 **and humoral responses in the female reproductive tract, the main**  
4 **HIV portal of entry**

5

6 **Running Head**

7 Mucosal vaccine responses in female genital tract

8

9 **Authors**

10 Romain Marlin<sup>\*,†,‡</sup>, Marie-Thérèse Nugeyre<sup>\*,†,‡</sup>, Nicolas Tchitchek<sup>\*</sup>, Matteo Parenti<sup>\*</sup>, Hakim

11 Hocini<sup>‡,§</sup>, Fahd Benjelloun<sup>\*,†</sup>, Claude Cannou<sup>\*,†</sup>, Nathalie Dereuddre-Bosquet<sup>\*</sup>, Yves Levy<sup>‡,§,¶</sup>,

12 Françoise Barré-Sinoussi<sup>‡,||</sup>, Gabriella Scarlatti<sup>‡,#</sup>, Roger Le Grand<sup>\*,‡</sup>, Elisabeth Menu<sup>\*,†,‡</sup>

13

14 <sup>\*</sup>Immunology of viral infections and autoimmune diseases/IDMIT Infrastructure/CEA/DRF/iMETI, Université  
15 Paris Sud, Inserm U 1184, Fontenay-Aux-Roses, France

16 <sup>†</sup> MISTIC group, department of Virology, Institut Pasteur, Paris, France

17 <sup>‡</sup> VACCINE RESEARCH INSTITUTE – VRI, Hôpital Henri Mondor, Créteil, France

18 <sup>§</sup> Université Paris-Est, Faculté de Médecine, INSERM U955, Créteil, France

19 <sup>¶</sup> Assistance Publique-Hôpitaux de Paris (AP-HP), Groupe Henri-Mondor Albert-Chenevier, Service  
20 d'immunologie clinique, Créteil, France

21 <sup>||</sup> International division, Institut Pasteur, Paris, France

22 <sup>#</sup> Viral Evolution and Transmission Unit, San Raffaele Scientific Institute, Milan, Italy

23

24 **Corresponding author**

25 Elisabeth Menu

26 Center for Immunology of Viral Infections and Autoimmune diseases (ImVA)

27 Building 02- 4th floor

28 18 route du Panorama  
29 92265 Fontenay-aux-Roses, France  
30 +33 1 46 54 83 14  
31 Elisabeth.menu@pasteur.fr  
32

33 **Abstract**

34 The female reproductive tract is one of the major mucosal invasion site of HIV-1. This site has  
35 been neglected in previous HIV-1 vaccine studies. Immune responses in the female  
36 reproductive tract after systemic vaccination remain to be characterized. Using a modified  
37 vaccinia virus Ankara (MVA) as a vaccine model, we characterized specific immune responses  
38 in all compartments of the female reproductive tract (FRT) of non-human primates after  
39 systemic vaccination. Memory T cells were preferentially found in the lower tract (vagina and  
40 cervix), whereas antigen-presenting cells and innate lymphoid cells were mainly located in the  
41 upper tract (uterus and fallopian tubes). This compartmentalization of immune cells in the FRT  
42 was supported by transcriptomic analyses and correlation network. Polyfunctional MVA-  
43 specific CD8<sup>+</sup> T cells were detected in the blood, lymph nodes, vagina, cervix, uterus and  
44 fallopian tubes. Anti-MVA IgG and IgA were detected in cervicovaginal fluid after a second  
45 vaccine dose. Systemic vaccination with an MVA vector thus elicits cellular and antibody  
46 responses in the female reproductive tract.

47

48 ***Introduction***

49 Heterosexual intercourse is the major route of HIV-1 transmission(1), and viral entry occurs  
50 mainly via the female reproductive tract (FRT) mucosae. One of the attempts to prevent this  
51 transmission should focus on inducing mucosal immune responses.

52 The FRT contains two types of mucosae. The type I mucosal surface is found in the upper  
53 genital tract (endocervix, uterus and Fallopian tubes), and is covered by a monolayer of  
54 columnar epithelial cells with tight junctions. The type II mucosal surface is found in the lower  
55 genital tract (vagina and ectocervix), and is lined with a stratified squamous epithelium. The  
56 boundary between the type I and II mucosae is called the cervical transformation zone. The  
57 transformation zone is considered to be more vulnerable to HIV-1 infection(2, 3), owing to the  
58 abundance of immune target cells (CD4<sup>+</sup> T cells, macrophages and dendritic cells), and the  
59 transition of the epithelial phenotype. Macrophages and T cells from the vagina and cervix are  
60 permissive to HIV-1 infection *in vitro*(4, 5). The uterus contains CD4<sup>+</sup> T cells and macrophages  
61 that express HIV-1 coreceptors. Uterine cells and uterine explants are also permissive to HIV-  
62 1 infection *in vitro*(6). Thus, as HIV-1 target cells are present throughout the FRT, an effective  
63 vaccine should induce protective responses in all FRT compartments.

64 Recombinant poxviruses such as vaccinia virus and canarypox virus are strongly immunogenic  
65 and are often used as vaccine vectors. Partial but significant protection against HIV-1 was  
66 observed in the Thai phase III trial (RV144) of a canarypox vector expressing HIV-1 antigens  
67 plus a trimeric recombinant gp120 protein, used in a prime/boost strategy(7). The modified  
68 vaccinia virus Ankara (MVA), another recombinant poxvirus, is widely used in vaccines for  
69 infectious diseases(8). Mucosal immunity after MVA vaccination has been studied in the  
70 gastrointestinal tract but not in the FRT(9).

71 Most studies of vaccine responses in the FRT have been performed in mice(10). However,  
72 macaques, which exhibit marked immunological and anatomical similarities to humans in  
73 contrast to mice(11), is the reference model for HIV-1 research and vaccine studies.

74 Here, using an MVA vaccine as a model, we examined whether systemic MVA vaccination  
75 induced specific local responses in the macaque FRT. After detailed phenotypic  
76 characterization of immune cell subpopulations, we examined specific immune responses in  
77 the blood, lymph nodes (LNs), vagina, cervix (endo and ecto), uterus and fallopian tubes.

78

## 79 ***Materials and Methods***

### 80 **Ethics statement**

81 Six sexually mature adult female cynomolgus macaques (*Macaca fascicularis*) imported from  
82 Mauritius were housed in the Infectious Disease Models and Innovative Therapies (IDMIT)  
83 facilities at Commissariat à l’Energie Atomique et aux Energies Alternatives (CEA, Fontenay-  
84 aux-Roses, France). Treatment of non-human primates (NHP) at CEA complies with French  
85 national regulations (CEA authorization A 92-032-02), with the Standards for Human Care and  
86 Use of Laboratory Animals (OLAW Assurance number #A5826-01), and with European  
87 Directive 2010/63 (recommendation #9). Experiments were supervised by veterinarians in  
88 charge of the animal facility. This study was approved and accredited by the Comité d’Ethique  
89 en Expérimentation Animale du CEA (A14-080) and by the French Research Ministry. Animals  
90 were housed in pairs under controlled conditions of humidity, temperature and light (12-hour  
91 light/dark cycles). Water was available *ad libitum*. The animals were monitored and fed once  
92 or twice a day with commercial monkey chow and fruits, by trained personnel, and were  
93 provided with environmental enrichment including toys, novel foodstuffs and music, under the  
94 supervision of the CEA Animal Welfare Officer.

95

### 96 **Experimental design**

97 On day zero (D0) and D58, the macaques received two subcutaneous injections per time point  
98 in the right and left side of the upper back, delivering 2 x 1 ml of inoculum containing a total  
99 of  $4 \times 10^8$  plaque-forming units (PFU) of recombinant MVA-HIV-1 expressing the Gag, Pol,  
100 and Nef proteins from HIV-1 strain LAI (ANRS-MVA HIV-B, MVATG17401, Transgene Ltd,  
101 France). The animals were monitored daily for signs of disease, appetite loss and lethargy. A  
102 physical examination was performed at each blood sampling and each inoculation. All  
103 experimental procedures (handling, immunization, blood sampling) were conducted after

104 sedation with ketamine hydrochloride (Rhône-Mérieux, Lyon, France, 10 mg/kg). To  
105 synchronize their hormonal cycle, an intramuscular injection of a synthetic variant of  
106 progesterone (Depoprovera, 30mg, Pfizer, France) was given 42 days after the first vaccine  
107 injection. The animals were sedated 77 days after the first vaccine injection with ketamine  
108 hydrochloride (10 mg/kg) then euthanized by intravenous injection of 180 mg/kg sodium  
109 pentobarbital.

110

### 111 **Sample collection and cell isolation**

112 Blood, serum and vaginal fluid were collected before and after each vaccine inoculation and at  
113 the time of euthanasia. Lymph nodes (LNs) and tissues were collected at necropsy. Serum was  
114 isolated by centrifugation at 3000 rpm for 10 min and stored at -80°C. Cervicovaginal fluid was  
115 collected with a Weck-Cel spear (Medtronic, USA) placed in the vaginal vault for 2 minutes.  
116 Secretions were recovered from the spears by adding 600 µl of extraction buffer (PBS, NaCl  
117 0.25 M and protease inhibitor cocktail (Merck Millipore, Fontenay-sous-bois, France)) and then  
118 centrifuging at 13 000 g for 20 min. Filtered vaginal fluids were stored at -80°C.

119 PBMC were isolated in heparin CPT tubes (BD biosciences, Le Pont de Claix, France) after  
120 centrifugation for 30 min at 3000 rpm. PBMC were collected from the top of the CPT gel  
121 surface and washed twice. At euthanasia, LN and FRT tissues were collected. LN cells were  
122 obtained by mechanical dissociation. FRT tissues (vagina, cervix, uterus and fallopian tubes)  
123 were isolated and cut into small pieces. Each tissue was digested for 1 hour at 37°C with  
124 agitation in digestion buffer, consisting of RMPI 1640 (Fisher Scientific, Illkirch, France),  
125 collagenase IV (0.3 mg/ml, Sigma Aldrich, St Quantin Fallavier, France), fetal calf serum (5%,  
126 Fisher Scientific), HEPES (0.025 M, Fisher Scientific), DNase (0.1 mg/ml, Roche, Mannheim,  
127 Germany), and antibiotics (Fisher Scientific). Undigested pieces were subjected to up to 3 more  
128 digestion steps. Cell suspensions from LNs and FRT tissues were filtered through 70-µm sterile

129 nylon cell strainers (BD biosciences). The median of cell numbers recovered for each FRT  
130 compartment was  $14.2 \times 10^6$  cells/g of tissue (ie  $64 \times 10^6$  cells) in the vagina,  $13.8 \times 10^6$  cells/g of  
131 tissue (ie  $54 \times 10^6$  cells) in the cervix,  $15 \times 10^6$  cells/g of tissue (ie  $62 \times 10^6$  cells) in the uterus and  
132  $27.7 \times 10^6$  cells/g of tissue (ie  $18 \times 10^6$  cells) in the tubes.

133

#### 134 **Immune phenotyping**

135 Whole blood, LN cells and cells from FRT compartments were analyzed by flow cytometry.  
136 The cells were incubated with the antibodies listed in Table S1, then washed and fixed with  
137 FACS lysing buffer or BD Cell Fix solution. A Fortessa 2-UV 6-Violet 2-Blue 5-Yelgr 3-Red  
138 laser configuration was used (BD biosciences), with Diva (BD) and FlowJo 9.8.3 (Tristar, USA)  
139 softwares. At least 500 events for rare cell populations (i.e. pDC) were recorded. The gating  
140 strategies are illustrated in supplemental figure S1a-d.

141

#### 142 **Cellular responses**

143 Specific cellular immune responses were evaluated with *in vitro* stimulation assays. The cells  
144 were incubated for 5 hours at  $37^\circ\text{C}$  with medium, with 0.3 PFU/cell of live wild type MVA, or  
145 with PMA (5 ng/ml) and ionomycin (500 ng/ml) (Sigma Aldrich) in DMEM medium (Fisher  
146 Scientific) supplemented with 10% FCS and antibiotics. Brefeldin A was then added (5  $\mu\text{g/ml}$ ,  
147 Sigma Aldrich) and the cells were incubated for a further 10 hours at  $37^\circ\text{C}$ . For HIV-1  
148 stimulation, cells were incubated with 4  $\mu\text{g/ml}$  overlapping GAG peptide pools in DMEM  
149 medium supplemented with 10% FCS, antibiotics and costimulatory antibodies, for 1 hour at  
150  $37^\circ\text{C}$ , then for an additional 4 hours with brefeldin A (5  $\mu\text{g/ml}$ ). The cells were stained with  
151 blue dye (LIVE/DEAD® Fixable Blue Dead Cell Stain, Thermo Fisher) for viability then fixed  
152 and permeabilized with BD Fix&Perm reagent (BD Bioscience). The antibodies listed in Table  
153 S2 were used for intracellular staining. At least 5,000 events in the  $\text{CD8}^+$  T cell gate were

154 recorded. The gating strategy was as described elsewhere (12). Briefly, expression of cytokines  
155 and activation markers was evaluated in CD4<sup>+</sup> and CD8<sup>+</sup> T cells, and Boolean gate analyses  
156 were performed with FlowJo software. The percentages of cells positive for cytokines and  
157 activation markers were then compared between unstimulated and MVA- or GAG peptide pool-  
158 stimulated cells. Immune response was considered positive against the antigen when the  
159 percentage of cells positive for cytokines and activation markers were at least twice superior to  
160 the percentage under unstimulated condition.

161

### 162 **Antibody responses**

163 Specific antibodies were measured by EIA in serum and vaginal fluid collected by Weck-cel  
164 spears. 96-well MaxiSorp microplates (Nunc, Thermo Fisher) were coated overnight with 10<sup>5</sup>  
165 PFU/well wtMVA (Transgene, Illkirch, France) in NaHCO<sub>3</sub>/Na<sub>2</sub>CO<sub>3</sub> buffer, or with 1 µg/ml  
166 p24 antigen (kind gift from Bernard Verrier, LBTI UMR5305) in PBS. The plates were then  
167 blocked for 1 h with PBS containing 3% (w/v) bovine serum albumin (BSA, Sigma Aldrich) or  
168 with PBS containing 10% skimmed milk. The plates were washed 5 times with PBS containing  
169 0.1% Tween 20 and 10 mM EDTA, then incubated with two-fold serial dilutions of macaque  
170 fluids diluted in PBS containing 1% BSA for 1 h at RT (to detect anti-MVA IgG/IgA) or in  
171 PBS containing 1% skimmed milk and 0.05% Tween 20 for 1 h at 37°C (to detect anti-HIV  
172 IgG), starting at 1:50 for serum and 1:20 for vaginal fluid. The plates were then washed 5 times  
173 and incubated for 1 h with a 1:20,000 dilution of horseradish peroxidase-conjugated goat anti-  
174 monkey H+L chain IgG (Bio-Rad, Marne-la-Coquette, France) or with a 1:5,000 dilution of  
175 horseradish peroxidase-conjugated goat anti-monkey IgA (Alpha Diagnostic international, San  
176 Antonio, TX). The plates were washed five times, then 100 µL of o-phenylenediamine  
177 dihydrochloride (OPD) (Sigma Aldrich) was added and incubated for 30 mins at RT in the dark.  
178 The reaction was stopped by adding 2N H<sub>2</sub>SO<sub>4</sub>. Absorbance was measured at 492 nm with

179 spectrophotometer (Tecan, Lyon, France), and data were analyzed with Magellan software  
180 (Tecan). Antibody titers were calculated by extrapolation from the OD as a function of a serum  
181 dilution curve and were defined as the dilution of the test serum reaching 2 OD of the  
182 corresponding preimmune serum or vaginal fluid, tested at 1:50 and 1:30, respectively.

183

#### 184 **RNA extraction and hybridization**

185 Tissue biopsies collected at euthanasia were immediately immersed in RLT-beta-  
186 mercaptoethanol 1/100 lysis buffer (Qiagen, Courtaboeuf, France), then disrupted and  
187 homogenized with a TissueLyser LT (Qiagen). RNA was purified with Qiagen RNeasy  
188 microkits. Contaminating DNA was removed by using the RNA Cleanup step of the RNeasy  
189 microkit. Purified RNA was quantified with a ND-8000 spectrophotometer (NanoDrop  
190 Technologies, Fisher Scientific, Illkirch, France) before being checked for integrity on a 2100  
191 BioAnalyzer (Agilent Technologies, Massy, France). cDNA was synthesized and biotin-  
192 labelled using the Ambion Illumina TotalPrep RNA amplification kit (Applied  
193 Biosystem/Ambion, Saint-Aubin, France). Labelled cRNA was hybridized on Illumina Human  
194 HT-12V4 BeadChips, that target 47 323 probes corresponding to 34 694 genes. The  
195 manufacturers' protocols were followed.

196

#### 197 **Transcriptome analysis**

198 Microarray data were analyzed with R/Bioconductor software. Gene expression values were  
199 quantile normalized. Differentially expressed genes were identified with a paired non-  
200 parametric *t*-test ( $q$ -value $<0.05$ ), based on a fold-change cutoff of 1.2. Functional enrichment  
201 analysis used QIAGEN's Ingenuity Pathway Analysis (IPA, QIAGEN, Redwood City,  
202 [www.qiagen.com/ingenuity](http://www.qiagen.com/ingenuity)). Hierarchical clustering presented in the heatmaps were generated  
203 with the Euclidian metric and complete linkage methods. Microarray raw data are available

204 from the EBI-ArrayExpress database ([www.ebi.ac.uk/arrayexpress](http://www.ebi.ac.uk/arrayexpress)) under accession number E-  
205 MTAB-5663. The transcriptomic and cellular co-expression network was generated by using  
206 the Spearman correlation coefficients, based on the abundance of cell populations and  
207 normalized gene expression values across the whole dataset. Significant correlations ( $R > 0.70$   
208 and  $p\text{-value} < 0.01$ ) were restricted to correlations between cell populations, and between cell  
209 populations and gene expression levels.

210 **Results**

211

212 Characterisation of FRT leukocytes

213 To characterize the vaccine responses at the mucosal level, an extensive identification of the  
214 cell subpopulations present in the different compartments was first performed. The phenotypes  
215 of immune cells collected from FRT compartments and lymph nodes were analyzed by flow  
216 cytometry. The proportions of immune cell subsets were characterized in four sites of the FRT  
217 (vagina, cervix, uterus and tubes) by comparison with whole blood and both proximal and distal  
218 lymph nodes (iliac, axillary and inguinal). Leukocytes were present in all the FRT  
219 compartments (Figure 1a),

220 *-Innate immune cells*

221 Two subpopulations of innate lymphoid cells (ILC) were identified on the basis of  
222 NKG2A (NK cells) and NKp44 (ILC-3) expression (Supplementary Figure S1b). NK cells  
223 composed less than  $4.0 \pm 2.0\%$  (median  $\pm$  SD) of leukocytes in blood and LN. This percentage  
224 was higher in the FRT compartments, especially in the uterus ( $13.9 \pm 5.2\%$ ) (Figure 1b). The NK  
225 phenotype differed between the mucosae and blood, as mucosal NK cells did not express CD16  
226 Fc- $\gamma$  receptor but expressed CD69. In the LN and FRT, NKp44 was expressed by ILC-3 cells  
227 but not by NK cells (Figure 1c and Supplementary Figure S1b). Although few in number, ILC-  
228 3 cells were found in all LN and FRT compartments, and preferentially in the tubes ( $0.5 \pm 0.4\%$ )  
229 (Figure 1d).

230 The distribution of three main APC populations (CD14<sup>+</sup> APC, CD123<sup>+</sup> plasmacytoid  
231 dendritic cells (pDC) and CD11c<sup>+</sup> myeloid dendritic cells (mDC)) is shown in Supplementary  
232 Figure S1c accordingly to the gating strategy.

233 CD14<sup>+</sup> APC were the main APC subtype in all FRT compartments (Figure 1e) (from  $1.5 \pm 1.0\%$   
234 to  $5.3 \pm 5.6\%$  of total leukocytes) and were principally located in the uterus. The proportions of

235 these cells were similar in the lower FRT and blood, but only mucosal CD14<sup>+</sup> cells expressed  
236 the activation marker CD69 and the Fc- $\gamma$  receptor CD16, particularly in the vagina (Figure 1f).  
237 The distribution of mDC (CD11c<sup>+</sup>) was similar to that of CD14<sup>+</sup> cells, and mDC were mainly  
238 found in the uterus (3.4 $\pm$ 2.2% of total leukocytes) (Figure 1g). The proportion of pDC  
239 (CD123<sup>+</sup>) was similar in all the compartments, where they represented less than 1% of total  
240 leukocytes (Figure 1h).  
241 Neutrophils were the main leukocyte subtype in blood (43.8 $\pm$ 14.1% of CD45<sup>+</sup> cells). In the  
242 FRT, neutrophils were mainly found in the cervix and upper compartments (8.9 $\pm$ 6.8% in cervix,  
243 3.4 $\pm$ 1.8% in uterus and 2.3 $\pm$ 4.0 in the fallopian tubes) (Figure 1i).

#### 244 *-Antigen-specific immune cells*

245 T lymphocytes were the main leukocyte subpopulation in the LN and FRT  
246 compartments. The percentage of CD8<sup>+</sup> T cells in the FRT mucosae was higher than the  
247 percentage of CD4<sup>+</sup> T cells, contrasting with blood and LN (Figure 2a and 2d). CD4<sup>+</sup> T cells  
248 represented about 50% of total leukocytes in LN, nearly 20% in the lower FRT and 10% in the  
249 upper FRT (Figure 2a). The T cell memory phenotype was defined by CD28, CD95 and  
250 CD45RA expression (Supplementary Figure S1d). In contrast to blood and LN, the majority of  
251 CD4<sup>+</sup> T cells in the FRT exhibited the central memory phenotype (CD28<sup>+</sup>/CD95<sup>+</sup>), while naïve  
252 cells (CD28<sup>+</sup>/CD95<sup>neg</sup>) were rare (Figure 2b). In the FRT, up to 40% of leukocytes were CD8<sup>+</sup>  
253 T cells (Figure 2d). These cells expressed markers of central memory (CD28<sup>+</sup>/CD95<sup>+</sup>) and  
254 effector memory (CD28<sup>neg</sup>/CD95<sup>+</sup>), contrary to blood and LN, where most CD8 T cells were  
255 naïve (Figure 2e). Mucosal CD4<sup>+</sup> and CD8<sup>+</sup> T cells frequently expressed CD69 (Figures 2c and  
256 2f).

257 Between 6.7% and 15.9% of blood and LN leukocytes were B cells (CD20<sup>+</sup>)  
258 (Supplementary Figure S1d), whereas B cells were infrequent in all the FRT compartments  
259 (from 0.1 $\pm$ 0.1% to 1.0 $\pm$ 1.4% of leukocytes) (Figure 2g).

260 Thus, cells involved in initiating immune responses, and effector cells, were present  
261 throughout the macaque FRT, with specific distribution according to the compartment.

262

263 *Vaccine-specific CD4<sup>+</sup> T cells found mainly in lymph nodes draining the inoculation site*

264 The anti-MVA T cell response was monitored in blood by using an *in vitro* re-stimulation assay.  
265 Antigen-specific CD4<sup>+</sup> T cells were identified as CD154<sup>+</sup> cells. Their percentage increased in  
266 blood two weeks after the first and second vaccine injections (respectively 0.84% and 0.85%  
267 among total CD4<sup>+</sup> T cells; mean) (Figure 3a). Three weeks after the second vaccine injection,  
268 the anti-MVA response was analyzed in all compartments. Antigen-specific CD4<sup>+</sup> T cells were  
269 significantly detected in PBMC and LNs (Figure 3b). The largest percentage of MVA-specific  
270 CD4<sup>+</sup> T cells was found in the axillary LNs (from 0.23% to 3.24% of total CD4<sup>+</sup> T cells). No  
271 MVA-specific CD4<sup>+</sup> T cell response was detected in FRT tissue, as the percentage of CD154<sup>+</sup>  
272 CD4<sup>+</sup> T cells did not significantly change after MVA re-stimulation (Figure 3b). In all  
273 compartments, CD154<sup>+</sup> cells represented a large percentage of CD4<sup>+</sup> T cells after stimulation  
274 with PMA and ionomycin (data not shown). The anti-HIV-1 response was also analyzed after  
275 *in vitro* stimulation with gag peptide pools and co-stimulatory antibodies (anti-CD28 and anti-  
276 CD49d mAbs). The addition of co-stimulatory antibodies induced non-specific activation of T  
277 cells and thus increased background CD154 expression, even in non-stimulated conditions. As  
278 this could have masked weak responses, we measured the HIV-1-specific CD4<sup>+</sup> T cell response  
279 by analyzing the percentage of CD4<sup>+</sup> T cells that expressed CD154 and produced IFN- $\gamma$  (i.e.  
280 only specific T cells). The Gag-specific CD4<sup>+</sup> T cell response was very weak and only detected  
281 in PBMC (Figure 3c).

282 Thus, MVA-specific CD4<sup>+</sup> T cells were mainly found in blood and in lymph nodes draining the  
283 vaccine inoculation site.

284

285 Systemic and mucosal polyfunctional vaccine-specific CD8<sup>+</sup> T cell responses

286 Like the CD4<sup>+</sup> T cell response, the vaccine response mediated by CD8<sup>+</sup> T cells was monitored  
287 by *in vitro* re-stimulation assays in blood over time, and in all compartments at euthanasia. The  
288 percentage of MVA-specific CD8<sup>+</sup> T cells that produced IFN- $\gamma$  increased in blood after the first  
289 vaccine inoculation and rose strongly after the second injection (respectively 1.79% and 5.38%  
290 of total CD8<sup>+</sup> T cells; mean) (Figure 4a). A similar profile was observed for MIP-1 $\beta$  and TNF-  
291  $\alpha$  production by antigen-specific CD8<sup>+</sup> T cells over time (data not shown). MVA-specific CD8<sup>+</sup>  
292 T cells were detected in PBMC and LNs of all animals three weeks after the second vaccine  
293 injection. They represented from 0.15% to 7.16% of total CD8<sup>+</sup> T cells, depending on the animal  
294 (Figure 4b-c). Interestingly, MVA-specific CD8<sup>+</sup> T cell responses were also detected in all FRT  
295 compartments (Figure 4b and 4d) and especially in the vagina (from 0.04% to 1.08% of total  
296 CD8<sup>+</sup> T cells for the IFN- $\gamma$  response). The anti-MVA response mediated by CD8<sup>+</sup> T cells was  
297 polyfunctional. Importantly, most of the CD8<sup>+</sup> T cells which had only one function (produced  
298 one cytokine/chemokine) secreted MIP-1 $\beta$ , while those with two functions produced MIP-1 $\beta$   
299 and IFN- $\gamma$ , and those with three functions produced MIP-1 $\beta$ , IFN- $\gamma$  and TNF- $\alpha$  (Figure 4e).  
300 MVA-specific CD8<sup>+</sup> T cells from the FRT produced less TNF- $\alpha$  than their blood and LN  
301 counterparts (Figure 4c-e).

302 HIV-1 antigen-specific CD8<sup>+</sup> T cells were also measured in the different compartments. The  
303 background signal was high in all conditions, as noted for CD4<sup>+</sup> T cell responses. To detect  
304 HIV-1 antigen-specific CD8<sup>+</sup> T cells, the analyses focused on CD8<sup>+</sup> T cells which produced  
305 both MIP-1 $\beta$  and IFN- $\gamma$ . Anti-gag CD8<sup>+</sup> T cells were detected above background in one animal's  
306 PBMC (triangle), LNs and uterus (Fig. 4f).

307 Thus, MVA-specific CD8<sup>+</sup> T cell responses were polyfunctional and found in all FRT  
308 compartments, in addition to blood and LNs.

309

310 Vaccine-specific IgG and IgA detected in vaginal fluid after the second vaccine inoculation.

311 To analyze humoral responses, vaccine-specific Ig titers were serially determined in serum and  
312 vaginal fluid by ELISA. MVA-specific IgG was detected in all the animals' sera two weeks  
313 after the first and second vaccine inoculations (respective titers of  $1,216 \pm 430$  and  $50,079 \pm 11$   
314  $780$ ; mean of 6 animals) (Figure 5a), and in vaginal fluid only after the second inoculation (titer  
315 of  $634 \pm 386$ , mean of 6 animals) (Figure 5b). Similarly, MVA-specific IgA was detected in  
316 serum after the two vaccine inoculations (respective titers of  $282 \pm 250$  and  $1,960 \pm 1532$ , mean  
317 of 6 animals) and in vaginal fluid only after the second inoculation (titer of  $231 \pm 132$ , mean of  
318 6 animals) (Figure 5c-d). The anti-HIV-1 humoral response was estimated by measuring Gag-  
319 specific IgG (Figure 5e-f). These antibodies were detected in the serum of 4 of 6 animals after  
320 the first vaccine inoculation, and in all 6 animals' serum after the second inoculation. In contrast,  
321 Gag-specific IgG was not detected in vaginal fluid (Figure 5f).

322 Thus, systemic MVA vaccination induced detectable vector-specific IgG and IgA in vaginal  
323 fluid after the second vaccine injection.

324

325 Transcriptomic analyses highlight FRT compartmentalization of immune cells

326 To better characterize the events at the molecular level, we compared the transcriptomic  
327 profiles from vaginal, cervical and uterine tissue samples. The numbers of differentially  
328 expressed genes (DEG) in each comparison are represented in Figure 6a. We found that  
329 respectively 3,810 and 4,800 genes were differentially expressed in the cervix and uterus  
330 compared to vagina. We identified 3,804 DEG in the uterus versus the cervix. The Venn  
331 diagram in Figure 6b represents the common DEG between the comparisons, showing that 624  
332 genes were shared between the three comparisons (i.e. cervix vs vagina, uterus vs vagina and  
333 uterus vs cervix). The relative expression of genes found as DEG in at least one comparison is  
334 represented by a heatmap in Figure 6c. Four main branches (gene clusters) were identified by

335 hierarchical clustering. The clustering branch #2 was mainly driven by DEGs over-expressed  
336 in the uterus. Similarly, branch #1 was driven by DEGs over-expressed in the vagina, while  
337 branches #3 and #4 were driven by DEGs over-expressed in the cervix. Each gene set was  
338 analyzed using Ingenuity Pathway Analysis (IPA). Branches #3 and #4 were merged for the  
339 enrichment analysis. Functional enrichment analysis of canonical pathways and upstream  
340 regulators are represented on the side of each branch. Upstream regulator analyses highlighted  
341 that beta-estradiol (branch #1  $p=9.69e^{-30}$ ; branch #2  $p=2.7e^{-21}$ ; branches #3-4  $p=8.39e^{-8}$ ),  
342 progesterone (branches #3-4  $p=1.16e^{-10}$ ) and estrogen receptor (ESR1) (branch #2  $p=8.77e^{-17}$ ;  
343 branches #3-4  $p=1.45e^{-10}$ ) constituted top upstream regulators in at least one of the four  
344 branches, confirming that hormones are involved in central regulation pathways in the FRT.

345 Enrichment analyses were then filtered to reveal immune-related pathways. Significant  
346 immune-related canonical pathways and associated p-values are represented in Figure 6d. The  
347 results showed that numerous pathways are associated with the uterus (branch #2) and are  
348 linked to NK cells and antigen-presenting cells (natural killer cell signaling  $p=8.51e^{-4}$ ; IL-15  
349 signaling  $p=2.04e^{-3}$ ; Crosstalk between dendritic cells and natural killer cells  $p=2.04e^{-3}$ ;  
350 production of nitric oxide and reactive oxygen species by macrophages  $p=9.77e^{-4}$ ). Similarly,  
351 in the vagina (branch #1), immune canonical pathways are associated with  
352 macrophages/monocytes and T cells (CTLA4 signaling in cytotoxic T cell  $p=2e^{-4}$ ; TCR  
353 signaling  $p=4.47e^{-3}$ ; Fc $\gamma$ -R mediated phagocytosis in macrophages and monocytes  $p=9.12e^{-4}$ ;  
354 CCR5 signaling in macrophages  $p=4.57e^{-3}$ ). No significant immune-related pathway was  
355 identified for the cervix (clustering branches #3 and #4).

356 To integrate flow cytometry and transcriptomic data, we generated a co-expression  
357 network. We restricted the correlations to DEG associated to the pathways in bold on Figure  
358 6D. Co-expression network revealed that frequent immune populations in the vagina (T and B  
359 cells) correlated positively with these branch #1 immune pathways and negatively with the

360 branch #2 immune pathways (Figure 6e). Conversely, frequent immune populations in the  
361 uterus (APC and ILC) correlated positively with the branch #2 immune pathways and  
362 negatively with the branch #1 immune pathways.  
363 Thus, transcriptome and correlation analyses highlighted the specificity of each FRT  
364 compartment and the compartmentalization of FRT immune cells.

365 ***Discussion***

366

367 As male-to-female transmission via the FRT mucosae is the main route of HIV-1 transmission,  
368 it is essential to study vaccine responses in the FRT. We conducted a detailed characterization  
369 of the immune cells involved in MVA-HIV-1 vaccine responses in the cynomolgus macaque,  
370 and the vaccine responses themselves in all female reproductive tract compartments during the  
371 luteal phase, by comparison with blood and draining lymph nodes. Previous studies of mucosal  
372 responses to MVA vaccination have been limited to the gastrointestinal tract(9), whereas the  
373 FRT is the main portal of entry for sexually transmitted pathogens. To our knowledge, we show  
374 for the first time that subcutaneous MVA injections induce specific immunoglobulin (IgG and  
375 IgA) and polyfunctional CD8<sup>+</sup> T cells in the FRT of female macaques. This study reveals that  
376 each FRT compartment has its own characteristics, as shown by immune cell phenotyping and  
377 transcriptomic analyses.

378

379 The first part of this study clearly shows that immune cells are compartmentalized. Two  
380 subpopulations of ILC were identified according to their phenotypes. Thus, NK cells, defined  
381 by NKG2A expression, were mainly found in the upper FRT (uterus and tubes) and expressed  
382 low levels of CD16 Fc- $\gamma$  receptor, as previously described (13), and no NKp44, in contrast to  
383 gut mucosae(14) (personal communication by Mariangela Cavarelli). Localization of NK cell  
384 activity within the uterus was confirmed by transcriptomic analyses, as NK cell-related  
385 pathways were associated with the uterus (branch #2) and correlated with uterine immune cell  
386 populations (co-expression network, Figure 6e). A second subtype of ILC, called ILC-3, which  
387 expressed NKp44 but not NKG2A(14), were also mainly found in the upper FRT.

388 We detected three main populations of professional APC, according to their phenotypic  
389 markers: i) CD14<sup>+</sup> APCs, ii) mDC that expressed CD11c<sup>+</sup>, and iii) plasmacytoid DC (pDC) that

390 expressed CD123<sup>+</sup>. These APCs were distributed throughout the FRT, but differences in their  
391 distribution and phenotype were noted. The largest percentage of mDC CD11c<sup>+</sup> cells and  
392 CD14<sup>+</sup> cells was found in the uterus. Moreover, phenotypic analyses of APC subtypes  
393 confirmed that CD14<sup>+</sup> APCs from the vagina expressed CD16 Fc- $\gamma$  receptor, contrary to  
394 intestinal CD14<sup>+</sup> APCs(15). This characteristic of vaginal CD14 APCs was supported by  
395 transcriptomic analysis, as the “Fc- $\gamma$  receptor-mediated phagocytosis in macrophages” pathway  
396 was enriched in the vagina.

397 B lymphocytes were the main leukocyte subtype in LNs, while they were detected at a very low  
398 percentage throughout the FRT, mainly in the vagina. This low frequency of B cells in the FRT  
399 was not due to the enzymatic digestion procedure, as very few B cells were detected by  
400 immunostaining of tissue biopsies (data not shown). Here, we detected B cells by their CD20  
401 expression rather than the CD19 marker usually used in humans, as the available antibodies do  
402 not cross-react in cynomolgus macaques. As CD20 is not expressed by all B cell subsets(16),  
403 this could explain the low percentage of B cells found in our samples. The distribution of  
404 CD20<sup>neg</sup> B cells such as plasma cells and antibody-secreting cells in FRT compartments will  
405 require further studies with specific markers.

406 T lymphocytes were the main immune cell populations in all the FRT compartments. CD8<sup>+</sup> T  
407 cells were more abundant than CD4<sup>+</sup> T cells within the mucosae, in contrast to blood and LNs.  
408 In particular, the vagina exhibited the largest percentage of CD8<sup>+</sup> T cells, as well as a specific  
409 transcriptomic signature related to T cell pathways. Co-expression networking showed that T  
410 cell abundance correlated positively with these T cell pathways (branch #1) (Figure 6e). We  
411 confirm that both CD4<sup>+</sup> and CD8<sup>+</sup> T cells express memory markers in the FRT(17), whereas  
412 naïve cells were mainly found in blood and LNs. Among the memory T cells, resident memory  
413 lymphocytes have been described in the tissues such as the vagina(18). Our analyses performed  
414 in one vaccinated animal showed that CD8<sup>+</sup> resident memory T cells were mainly present in

415 the vagina (39.8% among the effector memory T cells) and in the cervix (22.2% among the  
416 effector memory T cells) and were less frequent in the uterus (2.5% among the effector memory  
417 T cells) (data not shown). Together, these data show that immune cells exhibit tissue specificity  
418 in the macaque FRT.

419 Our results match some published data on the human FRT, including the observations that i)  
420 mucosal NK cells exhibit a unique phenotype and are mainly found in the uterus(19); ii) ILC-  
421 3 are detected in the upper FRT(20); iii) APCs are distributed throughout the FRT, particularly  
422 in the upper tract(21) and ectocervix(22); iv) CD20<sup>+</sup> B cells are rare throughout the FRT(23);  
423 v) memory CD8<sup>+</sup> T cells represent a large proportion of immune cells in all compartments of  
424 the human FRT. Thus, the localization and phenotype of immune cell subtypes are similar in  
425 the macaque and human FRT, validating the cynomolgus macaque as a model for human  
426 reproductive biology and genital immunity, including FRT mucosal immune responses to  
427 vaccination.

428 We therefore vaccinated female cynomolgus macaques subcutaneously with MVA-HIV-1,  
429 selected as a vaccine model, and analyzed specific responses in the FRT, LNs and blood.

430 Analyze of humoral responses confirmed that MVA vaccination induces strong anti-MVA IgG  
431 responses in serum, whereas anti-HIV IgG was not detected in all animals. In contrast to other  
432 mucosal fluids, cervicovaginal fluid contained more IgG than IgA. MVA-specific IgG and IgA  
433 were detected in vaginal fluid after the second vaccine injection. Local anti-MVA IgG titers  
434 were lower than in serum, as the vaccine was administered subcutaneously. Cervicovaginal IgG  
435 has been shown to come mainly from the systemic compartment(24). Anti-HIV IgG titers in  
436 serum were much lower than anti-MVA IgG titers, which could explain why anti-HIV IgG was  
437 not detected in vaginal fluid, given their systemic origin.

438 Anti-MVA responses mediated by CD4<sup>+</sup> T cells were weaker than those mediated by CD8<sup>+</sup> T  
439 cells in blood and LNs, and were not detectable in the FRT mucosae. Since the peak of CD4<sup>+</sup>

440 T cell responses precede the one of CD8<sup>+</sup> T cell responses(25), immune responses analysed 77  
441 days after the prime may not be optimal to detect a strong CD4<sup>+</sup> T cell response. The largest  
442 anti-MVA CD4<sup>+</sup> T cell responses were measured in axillary LNs, i.e. those draining the vaccine  
443 injection site (upper back). However, MVA-HIV vaccination may induce non-specific CD4<sup>+</sup> T  
444 cell activation, as CD4<sup>+</sup> T cells exhibited a high CD154 expression in some animals in  
445 unstimulated conditions.

446 Our study clearly shows that MVA vaccination induces strong specific CD8<sup>+</sup> T cell responses  
447 in blood, LNs and all FRT compartments. In the FRT, they were mainly localized in the vagina,  
448 but specific responses were also detected in the cervix, uterus and tubes. Responses mediated  
449 by CD8<sup>+</sup> T cells were polyfunctional, as specific CD8<sup>+</sup> T cells positive for two or more  
450 cytokines were detected. Boolean gating analyses were used to sort specific CD8<sup>+</sup> T cells  
451 according to the number of functions they displayed (single, double, triple or quadruple  
452 cytokine producers). The majority of single producer cells were MIP-1β<sup>+</sup>, double producers  
453 were MIP-1β<sup>+</sup> and IFN-γ<sup>+</sup>, triple producers were MIP-1β<sup>+</sup>, IFN-γ<sup>+</sup> and TNF-α<sup>+</sup>. These findings  
454 correspond to reports of blood CD8<sup>+</sup> T cell responses(26). TNF-α and IL-2 are thus produced  
455 only by highly polyfunctional cells. We noted that percentage of triple producer cells was lower  
456 in the FRT than in blood and LNs. Together, these results demonstrate that TNF-α<sup>+</sup> specific  
457 CD8<sup>+</sup> T cells are less abundant in the FRT than in blood and LNs.

458 Previous study has demonstrated that the MVA-HIV-1 vaccine induced T cell responses mainly  
459 against Gag and Pol genes(27). Due to limited amount of mucosal cells recovered to perform  
460 the different experiments and antigen stimulations, cellular and humoral immune responses  
461 induced against the HIV-1 insert in our present study were focused on anti-Gag responses. HIV-  
462 1 (Gag)-specific responses were mediated by CD4<sup>+</sup> T cells and were detected mainly in blood.  
463 These responses were weaker than MVA-specific CD8<sup>+</sup> T cell responses and were not  
464 detectable in the FRT, apart from the uterus of one animal. The MVA-HIV-1 vaccine was used

465 in this study as a model, and animals were vaccinated subcutaneously with two injections of  
466 the same vaccine construct. Therefore, specific responses mainly targeted the immunogenic  
467 vector. To enhance insert-specific responses, it will be essential for the boost or the prime to  
468 use another type of vaccine construct, such as a DNA vaccine, in addition to MVA(27).

469 The local environment of the FRT mucosae is under the influence of several factors, including  
470 hormones during the menstrual cycle, semen during intercourse, and sexually transmitted  
471 pathogens(28–30). As these factors impact mucosal immune cells and their environment, it will  
472 be crucial to study their possible influence on mucosal vaccine responses.

473 **Acknowledgment**

474 The authors thank Drs Anne-Sophie Beignon, Antonio Cosma, Mireille Centlivre and the Bmuc  
475 division members for scientific discussions, D. Young for critical editing of the manuscript,  
476 Transgene for providing the wild type MVA strain and ANRS/INSERM and the Vaccine  
477 Research Institute the MVA-HIV-B vaccine, the IDMIT core facilities for animal interventions  
478 and sampling, Rahima Yousfi for technical assistance and Dr Bernard Verrier for providing the  
479 p24 HIV-1 antigen.

480 **References**

- 481 1. Hladik, F., and M. J. McElrath. 2008. Setting the stage: host invasion by HIV. *Nat. Rev.*  
482 *Immunol.* 8: 447–57.
- 483 2. Li, Q., J. D. Estes, P. M. Schlievert, L. Duan, A. J. Brosnahan, P. J. Southern, C. S. Reilly,  
484 M. L. Peterson, N. Schultz-Darken, K. G. Brunner, K. R. Nephew, S. Pambuccian, J. D.  
485 Lifson, J. V Carlis, and A. T. Haase. 2009. Glycerol monolaurate prevents mucosal SIV  
486 transmission. *Nature* 458: 1034–8.
- 487 3. Pudney, J., A. J. Quayle, and D. J. Anderson. 2005. Immunological Microenvironments in  
488 the Human Vagina and Cervix: Mediators of Cellular Immunity Are Concentrated in the  
489 Cervical Transformation Zone. *Biol. Reprod.* 73: 1253–1263.
- 490 4. Shen, R., H. E. Richter, and P. D. Smith. 2011. Early HIV-1 target cells in human vaginal  
491 and ectocervical mucosa. *Am. J. Reprod. Immunol.* 65: 261–7.
- 492 5. Gupta, P., K. B. Collins, D. Ratner, S. Watkins, G. J. Naus, D. V Landers, and B. K.  
493 Patterson. 2002. Memory CD4(+) T cells are the earliest detectable human immunodeficiency  
494 virus type 1 (HIV-1)-infected cells in the female genital mucosal tissue during HIV-1  
495 transmission in an organ culture system. *J. Virol.* 76: 9868–76.
- 496 6. Quillay, H., H. El Costa, R. Marlin, M. Duriez, C. Cannou, F. Chrétien, H. Fernandez, A.  
497 Lebreton, J. Ighil, O. Schwartz, F. Barré-Sinoussi, M.-T. Nugeyre, and E. Menu. 2015.  
498 Distinct Characteristics of Endometrial and Decidual Macrophages and Regulation of Their  
499 Permissivity to HIV-1 Infection by SAMHD1. *J. Virol.* 89: 1329–1339.
- 500 7. Rerks-Ngarm, S., P. Pitisuttithum, S. Nitayaphan, J. Kaewkungwal, J. Chiu, R. Paris, N.  
501 Prensri, C. Namwat, M. de Souza, E. Adams, M. Benenson, S. Gurunathan, J. Tartaglia, J. G.  
502 McNeil, D. P. Francis, D. Stablein, D. L. Birx, S. Chunsuttiwat, C. Khamboonruang, P.  
503 Thongcharoen, M. L. Robb, N. L. Michael, P. Kunasol, J. H. Kim, and MOPH-TAVEG  
504 Investigators. 2009. Vaccination with ALVAC and AIDSVAX to Prevent HIV-1 Infection in

- 505 Thailand. *N. Engl. J. Med.* 361: 2209–2220.
- 506 8. Gilbert, S. C. 2013. Clinical development of Modified Vaccinia virus Ankara vaccines.  
507 *Vaccine* 31: 4241–4246.
- 508 9. Perreau, M., H. C. Welles, A. Harari, O. Hall, R. Martin, M. Maillard, G. Dorta, P.-A. Bart,  
509 E. J. Kremer, J. Tartaglia, R. Wagner, M. Esteban, Y. Levy, and G. Pantaleo. 2011.  
510 DNA/NYVAC vaccine regimen induces HIV-specific CD4 and CD8 T-cell responses in  
511 intestinal mucosa. *J. Virol.* 85: 9854–9862.
- 512 10. Gherardi, M. M., and M. Esteban. 2005. Recombinant poxviruses as mucosal vaccine  
513 vectors. *J. Gen. Virol.* 86: 2925–2936.
- 514 11. Wood, C. E. 2008. Morphologic and Immunohistochemical Features of the Cynomolgus  
515 Macaque Cervix. *Toxicol. Pathol.* 36: 119S–129S.
- 516 12. Guenounou, S., N. Bosquet, C. J. Dembek, R. Le Grand, and A. Cosma. 2013. OMIP-016:  
517 Characterization of antigen-responsive macaque and human T-cells. *Cytom. Part A* 83A: 182–  
518 184.
- 519 13. Reeves, R. K., J. Gillis, F. E. Wong, Y. Yu, M. Connole, and R. P. Johnson. 2010. CD16-  
520 natural killer cells: enrichment in mucosal and secondary lymphoid tissues and altered  
521 function during chronic SIV infection. *Blood* 115: 4439–4446.
- 522 14. Reeves, R. K., P. A. Rajakumar, T. I. Evans, M. Connole, J. Gillis, F. E. Wong, Y. V.  
523 Kuzmichev, A. Carville, and R. P. Johnson. 2011. Gut inflammation and indoleamine  
524 deoxygenase inhibit IL-17 production and promote cytotoxic potential in NKp44  
525 + mucosal NK cells during SIV infection. *Blood* 118: 3321–3330.
- 526 15. Shen, R., H. Richter, R. Clements, L. Novak, K. Huff, D. Bimczok, S. Sankaran-Walters,  
527 S. Dandekar, P. R. Clapham, L. E. Smythies, and P. D. Smith. 2009. Macrophages in Vaginal  
528 but Not Intestinal Mucosa Are Monocyte-Like and Permissive to Human Immunodeficiency  
529 Virus type 1 Infection. *J. Virol.* 83: 3258–3267.

- 530 16. Vugmeyster, Y., K. Howell, A. Bakshi, C. Flores, O. Hwang, and K. McKeever. 2004. B-  
531 cell subsets in blood and lymphoid organs in *Macaca fascicularis*. *Cytom. Part A* 61: 69–75.
- 532 17. Schultheiss, T., N. Stolte-Leeb, S. Sopper, and C. Stahl-Hennig. 2011. Flow cytometric  
533 characterization of the lymphocyte composition in a variety of mucosal tissues in healthy  
534 rhesus macaques. *J. Med. Primatol.* 40: 41–51.
- 535 18. Adnan, S., R. K. Reeves, J. Gillis, F. E. Wong, Y. Yu, J. V. Camp, Q. Li, M. Connole, Y.  
536 Li, M. Piatak, J. D. Lifson, W. Li, B. F. Keele, P. A. Kozlowski, R. C. Desrosiers, A. T.  
537 Haase, and R. P. Johnson. 2016. Persistent Low-Level Replication of SIV $\Delta$ nef Drives  
538 Maturation of Antibody and CD8 T Cell Responses to Induce Protective Immunity against  
539 Vaginal SIV Infection. *PLOS Pathog.* 12: e1006104.
- 540 19. Mselle, T. F., S. K. Meadows, M. Eriksson, J. M. Smith, L. Shen, C. R. Wira, and C. L.  
541 Sentman. 2007. Unique characteristics of NK cells throughout the human female reproductive  
542 tract. *Clin. Immunol.* 124: 69–76.
- 543 20. Montaldo, E., P. Vacca, L. Chiossone, D. Croxatto, F. Loiacono, S. Martini, S. Ferrero, T.  
544 Walzer, L. Moretta, and M. C. Mingari. 2016. Unique Eomes<sup>+</sup> NK Cell Subsets Are Present  
545 in Uterus and Decidua During Early Pregnancy. *Front. Immunol.* 6: 646.
- 546 21. Wira, C. R., J. V Fahey, C. L. Sentman, P. A. Pioli, and L. Shen. 2005. Innate and  
547 adaptive immunity in female genital tract: cellular responses and interactions. *Immunol.Rev.*  
548 206: 306–335.
- 549 22. Trifonova, R. T., J. Lieberman, and D. van Baarle. 2014. Distribution of immune cells in  
550 the human cervix and implications for HIV transmission. *Am. J. Reprod. Immunol.* 71: 252–  
551 64.
- 552 23. Lee, S. K., C. J. Kim, D.-J. Kim, and J.-H. Kang. 2015. Immune cells in the female  
553 reproductive tract. *Immune Netw.* 15: 16–26.
- 554 24. Russell, M. W., and J. Mestecky. 2002. Humoral immune responses to microbial

- 555 infections in the genital tract. *Microbes Infect.* 4: 667–677.
- 556 25. Blom, K., M. Braun, M. A. Ivarsson, V. D. Gonzalez, K. Falconer, M. Moll, H.-G.  
557 Ljunggren, J. Michaelsson, and J. K. Sandberg. 2013. Temporal Dynamics of the Primary  
558 Human T Cell Response to Yellow Fever Virus 17D As It Matures from an Effector- to a  
559 Memory-Type Response. *J. Immunol.* 190: 2150–2158.
- 560 26. Precopio, M. L., M. R. Betts, J. Parrino, D. A. Price, E. Gostick, D. R. Ambrozak, T. E.  
561 Asher, D. C. Douek, A. Harari, G. Pantaleo, R. Bailer, B. S. Graham, M. Roederer, and R. A.  
562 Koup. 2007. Immunization with vaccinia virus induces polyfunctional and phenotypically  
563 distinctive CD8(+) T cell responses. *J. Exp. Med.* 204: 1405–1416.
- 564 27. Dereuddre-Bosquet, N., M. L. Baron, V. Contreras, L. Gosse, I. Mangeot, F. Martinon, R.  
565 Yousfi, P. Clayette, Y. Levy, and R. Le Grand. 2015. HIV specific responses induced in  
566 nonhuman primates with ANRS HIV-Lipo-5 vaccine combined with rMVA-HIV prime or  
567 boost immunizations. *Vaccine* 33: 2354–2359.
- 568 28. King, A. E., K. Morgan, J. M. Sallenave, and R. W. Kelly. 2003. Differential regulation of  
569 secretory leukocyte protease inhibitor and elafin by progesterone. *Biochem. Biophys. Res.*  
570 *Commun.* 310: 594–599.
- 571 29. Hickey, D. K., M. V. Patel, J. V. Fahey, and C. R. Wira. 2011. Innate and adaptive  
572 immunity at mucosal surfaces of the female reproductive tract: stratification and integration of  
573 immune protection against the transmission of sexually transmitted infections. *J. Reprod.*  
574 *Immunol.* 88: 185–194.
- 575 30. Robertson, S. A. 2005. Seminal plasma and male factor signalling in the female  
576 reproductive tract. *Cell Tissue Res.* 322: 43–52.
- 577

578 **Footnotes**

579 This work was supported by French government “Programme d’Investissements d’Avenir”  
580 (PIA) under Grant ANR-11-INBS-0008 funding the Infectious Disease Models and Innovative  
581 Therapies (IDMIT, Fontenay-aux-Roses, France) infrastructure and PIA grants ANR-10-  
582 LABX-77 and ANR-10-EQPX-02-01 funding the Vaccine Research Institute (VRI, Créteil,  
583 France), the FlowCyTech facility, respectively. The authors declared no conflict of interest.

584

585 **Corresponding author**

586 Elisabeth Menu

587 Center for Immunology of Viral Infections and Autoimmune diseases (ImVA)

588 Building 02- 4th floor

589 18 route du Panorama

590 92265 Fontenay-aux-Roses, France

591 +33 1 46 54 83 14

592 Elisabeth.menu@pasteur.fr

593

594 **Figure legends**

595

596 Figure 1. Innate cell distribution in blood, LNs and FRT of vaccinated animals

597 (a) Distribution of leukocytes among living cells. Percentage of NK cells (b), ILC-3 (d), CD14<sup>+</sup>  
 598 cells (e), CD11c<sup>+</sup> mDC (g), CD123<sup>+</sup> pDC (h) and neutrophils (i) among leukocytes in the  
 599 different compartments. Each symbol represents one animal and the bar represents the median.  
 600 Phenotypic marker expression by NK cells (c) and CD14<sup>+</sup> cells (f) in the different compartments  
 601 are represented as a heat map. Each horizontal coloured line indicates one animal (n=6).

602

603 Figure 2. Adaptive immune cell distribution and phenotype

604 Percentage of CD4<sup>+</sup> T cells (a), CD8<sup>+</sup> T cells (d) and CD20<sup>+</sup> B cells (g) among CD45<sup>+</sup> cells in  
 605 the different compartments. Each symbol represents one animal and the bar represents the  
 606 median. Distribution of naïve (CD28<sup>+</sup>CD95<sup>-</sup>) and memory subsets (CM CD28<sup>+</sup>CD95<sup>+</sup>, EM  
 607 CD28<sup>-</sup>CD95<sup>+</sup>, EMRA CD28<sup>-</sup>CD95<sup>+</sup>CD45RA<sup>+</sup>) among CD4<sup>+</sup> (b) and CD8<sup>+</sup> (e) T cells (mean of  
 608 n=6). Histograms represent CD69 expression by CD4<sup>+</sup> (c) and CD8<sup>+</sup> (f) T cells in the different  
 609 tissues. (Mean +/- SEM of n=6)

610

611 Figure 3. Specific immune responses mediated by CD4<sup>+</sup> T cells

612 (a) Percentage of CD154<sup>+</sup> CD4<sup>+</sup> T cells over time in PBMC after *in vitro* stimulation with  
 613 medium (dotted lines) or wt MVA (full lines). Purple bold line indicates the mean of n=6 and  
 614 purple arrows indicate vaccine injections. (b) Percentage of CD154<sup>+</sup> CD4<sup>+</sup> T cells after *in vitro*  
 615 stimulation with medium (grey) or wt MVA (red) in the different compartments. (c) Percentage  
 616 of CD154<sup>+</sup>/IFN- $\gamma$ <sup>+</sup> CD4<sup>+</sup> T cells after *in vitro* stimulation with medium (grey) or gag peptide  
 617 pools (red) (GAG1 and GAG2) in blood and LNs (top panel c) and FRT mucosae (bottom panel  
 618 c). Each symbol represents one animal.

619

620 Figure 4. Vaccine-specific CD8<sup>+</sup> T cell responses in the blood, LNs and FRT

621 (a) Percentage of IFN- $\gamma$ <sup>+</sup> CD8<sup>+</sup> T cells over time in PBMC after *in vitro* stimulation with  
 622 medium (dotted lines) or wt MVA (full lines). Purple bold line indicates the mean of n=6 and  
 623 purple arrows indicate vaccine injections. (b) Dot plots of one representative animal ( $\nabla$ ) for  
 624 IFN- $\gamma$  staining after wt MVA stimulation in the different compartments. Percentages of IFN- $\gamma$ <sup>+</sup>  
 625 cells are indicated. (c-d) Percentage of IFN- $\gamma$ <sup>+</sup>, MIP-1 $\beta$ <sup>+</sup>, TNF- $\alpha$ <sup>+</sup> and IL-2<sup>+</sup> cells among CD8<sup>+</sup>  
 626 T cells after *in vitro* stimulation with medium (grey) or wt MVA (red) in blood and LNs (c) and  
 627 FRT tissues (d). (e) CD8<sup>+</sup> T cell polyfunction analysed by Boolean gating is represented as a  
 628 heat map. Each horizontal coloured line indicates one animal (n=6). (f) Percentage of MIP-1 $\beta$ <sup>+</sup>/  
 629 IFN- $\gamma$ <sup>+</sup> CD8<sup>+</sup> T cells after *in vitro* stimulation with medium (grey) or gag peptide pools (red)  
 630 (GAG1 and GAG2) in the different compartments. Each symbol represents one animal.

631

632 Figure 5. Specific humoral responses in serum and vaginal fluid of vaccinated animals

633 Titers of MVA (a-d)- and HIV-1 gag (e,f)-specific IgG and IgA over time in serum (a, c, e) and  
 634 vaginal fluid (b, d, f). Each symbol represents one animal, the bold line indicates the mean titer  
 635 of the six animals, and the dotted line indicates the detection limit. The purple arrows indicate  
 636 vaccine injections.

637

638 Figure 6. Transcriptomic profiling of vaginal, cervical and uterine tissues of vaccinated animals

639 (a) Bar charts showing the numbers of down-regulated (green) and up-regulated (red) genes in  
 640 comparison between vaginal, cervical and uterine tissues. (b) Venn diagram showing overlaps  
 641 between the set of differentially expressed genes found in the three comparisons. (c) Heatmap  
 642 showing the expression of the genes found to be differentially expressed in at least one  
 643 condition. Hierarchical clustering was performed at the gene level to identify 4 main sets

644 (clustering branches) of genes having similar expression profiles. Canonical pathways and  
645 upstream regulators found to be statistically over-represented in each clustering branch are  
646 indicated. (d) Immune-related canonical pathways and p-values associated with clustering  
647 branches #1 and #2. (e) Transcriptomic and cellular co-expression network. Each node of the  
648 graph corresponds to a biological variable and links between the nodes correspond to significant  
649 correlations (Spearman correlation coefficient). Genes are represented by circles and cell  
650 populations by squares. Gene circles are coloured based on their clustering branch associations  
651 (represented in (c) and (d)). Positive correlations are presented by red links and negative  
652 correlations by green links.

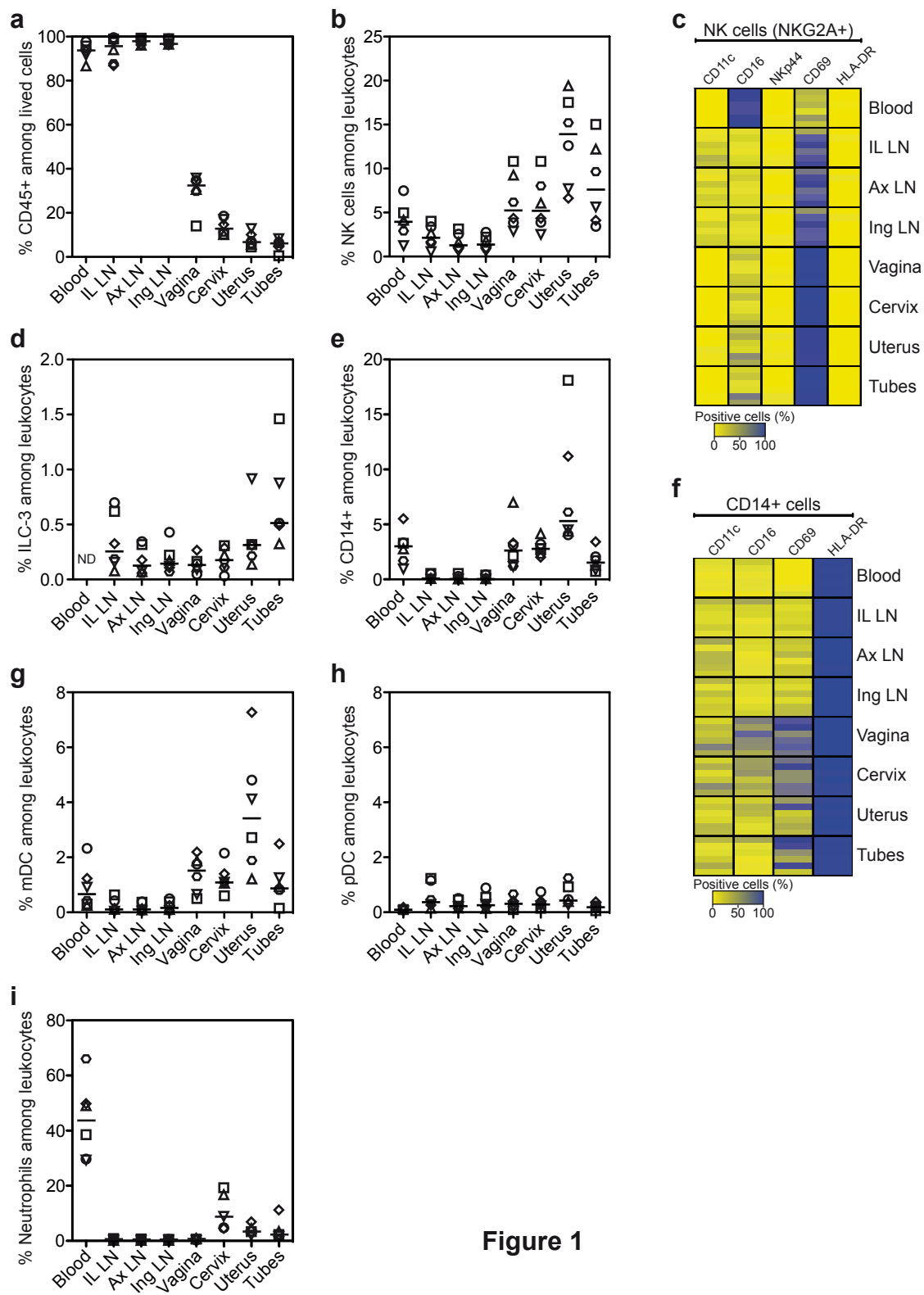
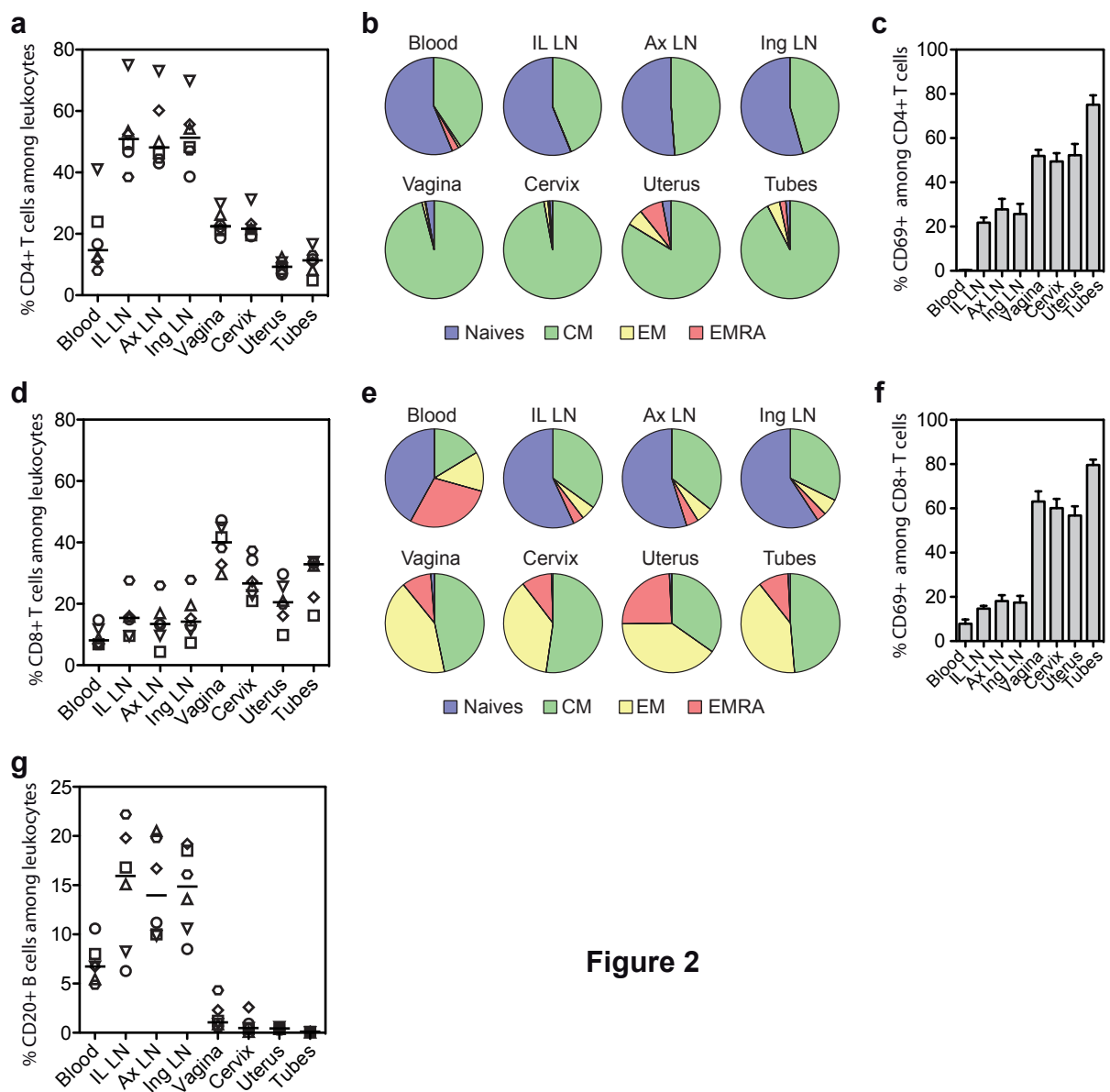
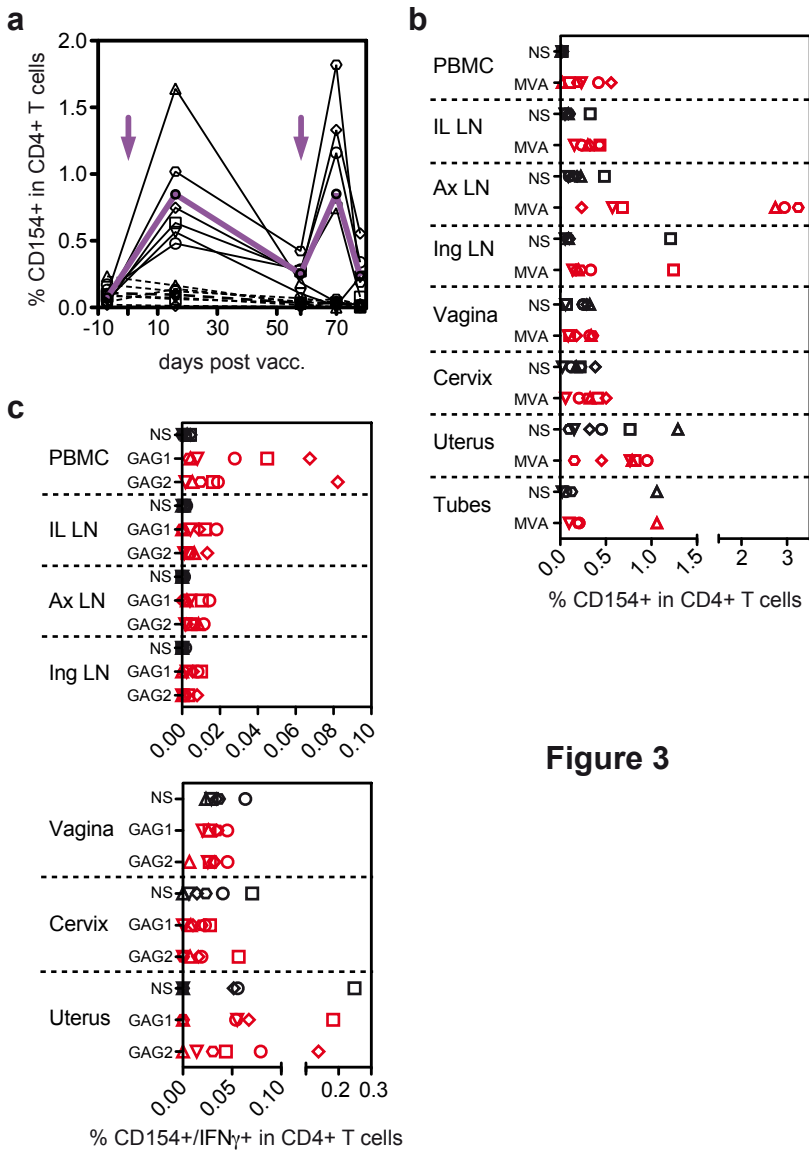


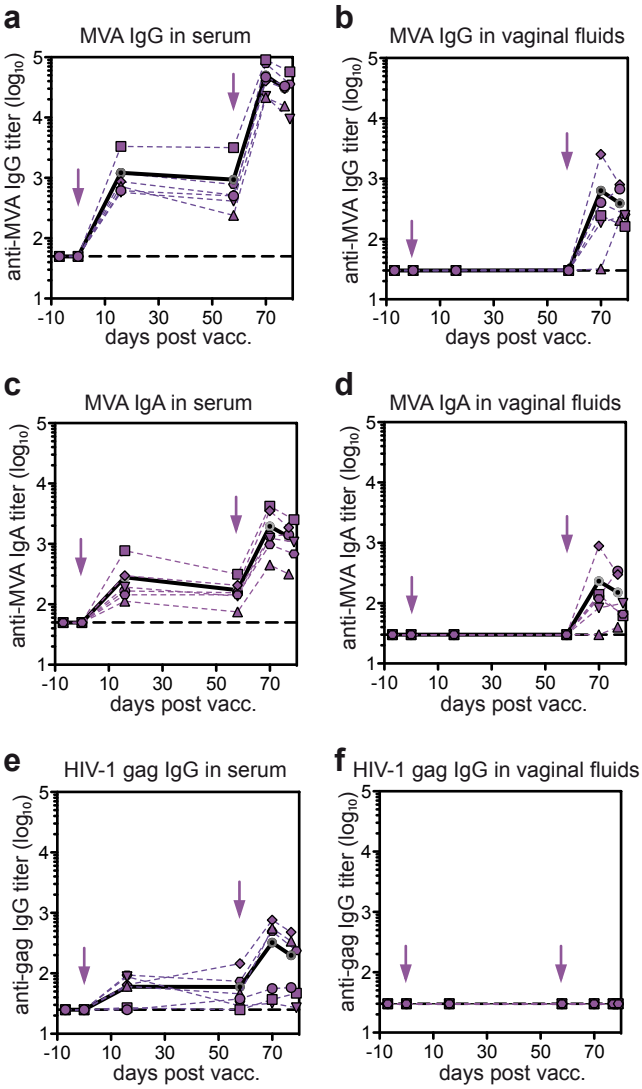
Figure 1



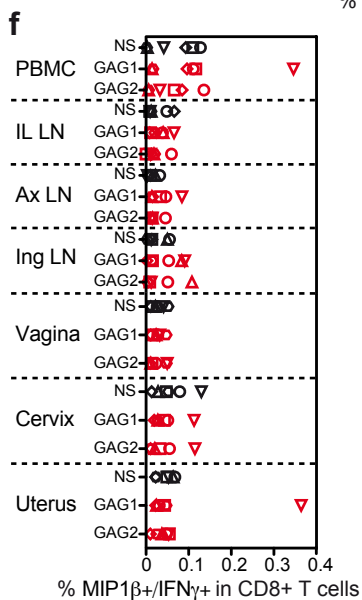
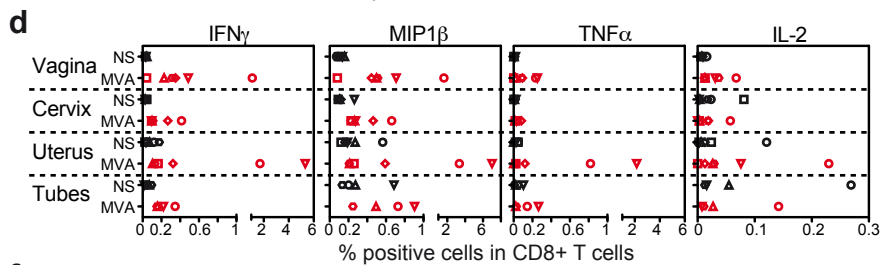
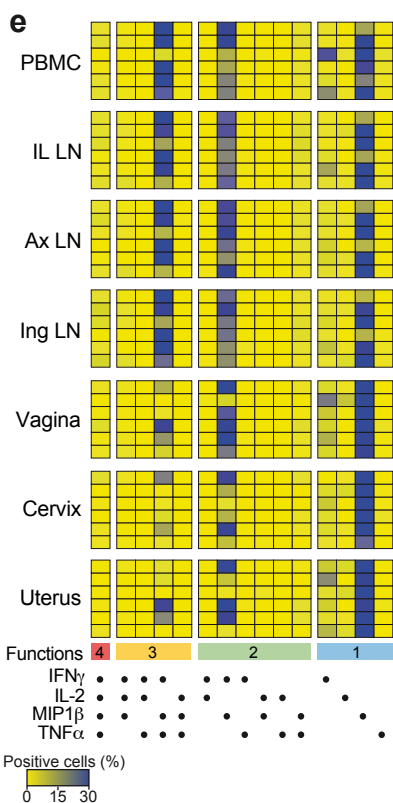
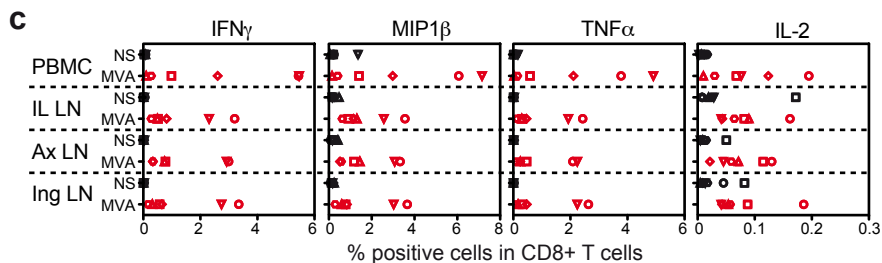
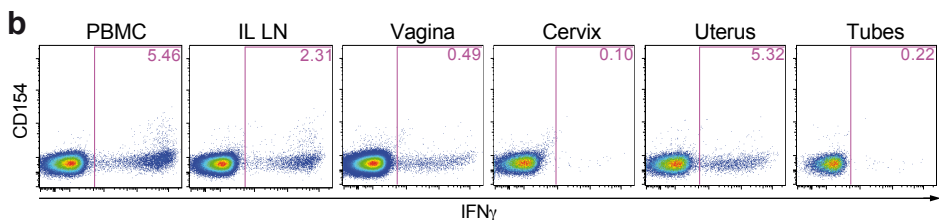
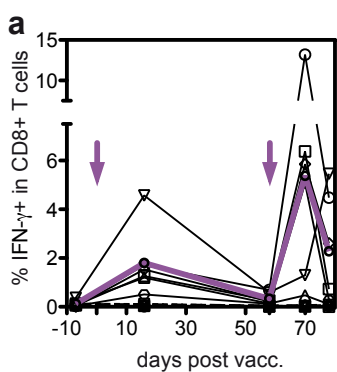
**Figure 2**

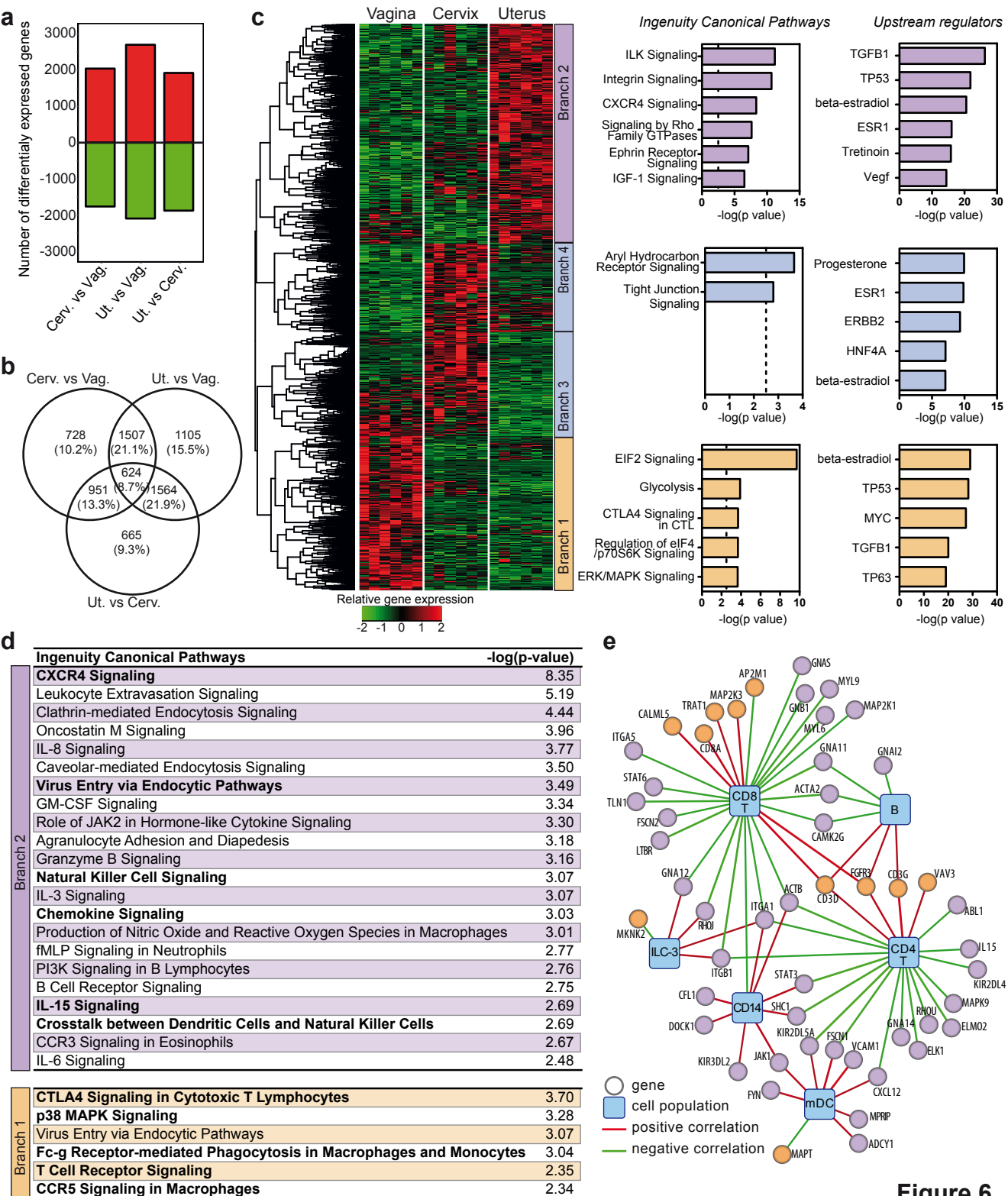


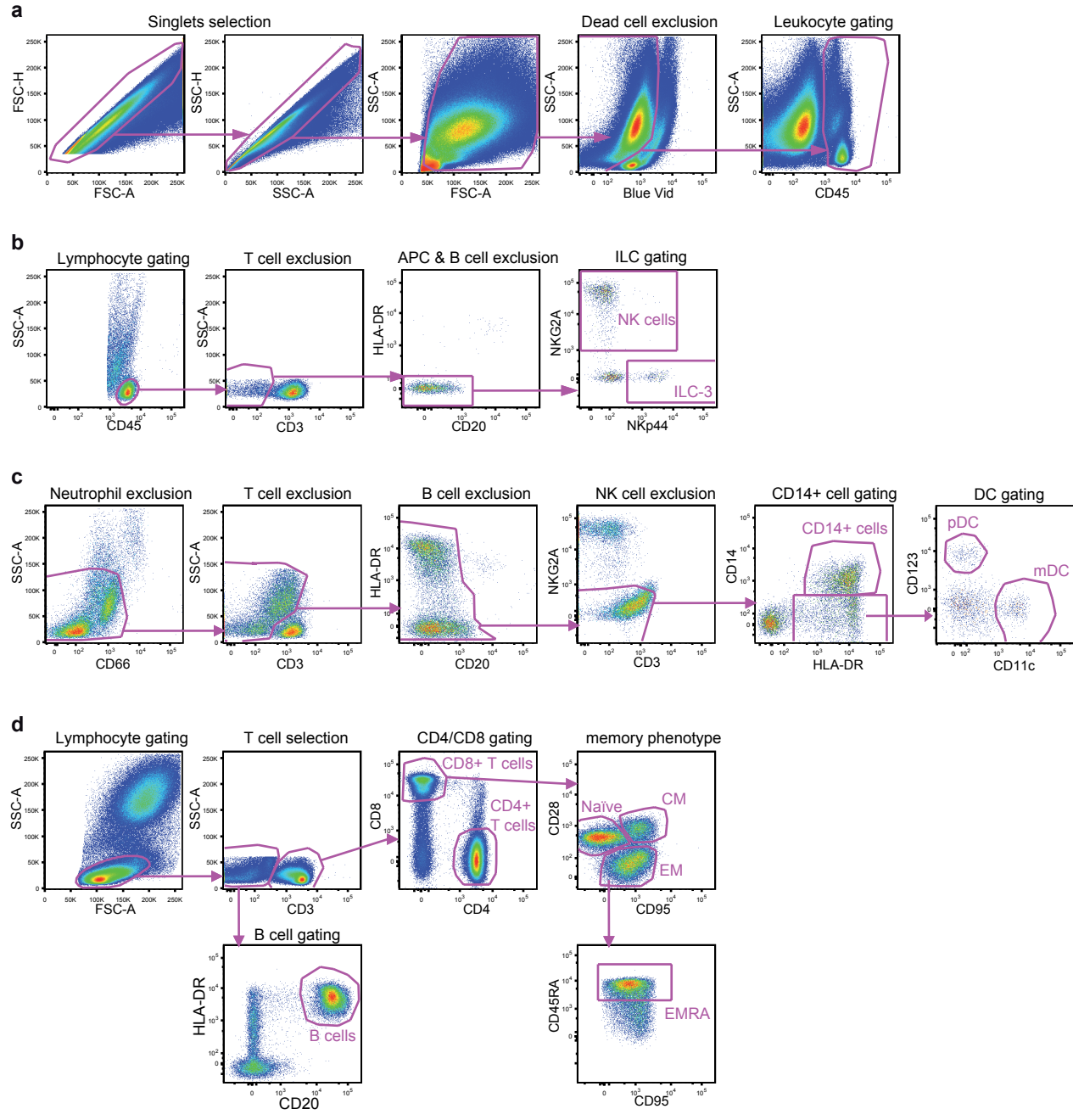
**Figure 3**



**Figure 5**







**Supplementary Figure 1. Gating strategy used to analyze immune cells.**  
 (a) Gating strategy used to analyze CD45+ leukocytes. The same strategy was applied to all the tissues and a representative illustration for the uterus is indicated. (b) ILC subsets were characterized after exclusion of T cells, B cells and APC (HLA-DR+ cells). NK cells are defined as NKG2A+ cells and ILC-3 as NKp44+ / NKG2Aneg cells. (c) APC subsets were defined as lineage negative and HLA-DR+ after exclusion of neutrophils, T cells, B cells and NK cells. (d) T cells are defined as CD3+ lymphocytes and B cells as CD20+ / HLA-DR+ lymphocytes. Memory subsets of CD4+ and CD8+ T cells were characterized by expression of CD28, CD95 and CD45RA markers.

Table SI. Antibodies used in immune phenotyping experiments.

| <b>Antibody</b> | <b>Fluorochrome</b> | <b>Clone</b> | <b>Supplier</b> |
|-----------------|---------------------|--------------|-----------------|
| <b>CD45</b>     | PerCp               | D058-1283    | BD pharmingen   |
| <b>CD3</b>      | V500                | SP34-2       | BD Horizon      |
| <b>CD4</b>      | V450                | L200         | BD Horizon      |
| <b>CD8</b>      | BV650               | RPA-T8       | BD Horizon      |
| <b>CD20</b>     | PE-CF594            | 2H7          | BD horizon      |
| <b>CD27</b>     | PE                  | MT-271       | BD pharmingen   |
| <b>CD45RA</b>   | PC7                 | L48          | BD              |
| <b>HLA-DR</b>   | APC-H7              | G46-6        | BD pharmingen   |
| <b>CD69</b>     | Alexa-700           | FN50         | BD pharmingen   |
| <b>CD21</b>     | BV711               | B-Ly4        | BD Horizon      |
| <b>CD28</b>     | FITC                | CD28,2       | BD pharmingen   |
| <b>CD95</b>     | APC                 | DX2          | BD pharmingen   |
| <b>CD20</b>     | BV711               | 2H7          | BD horizon      |
| <b>CD16</b>     | PE-CF594            | 3G8          | BD Horizon      |
| <b>NKG2A</b>    | PE                  | Z199         | Beckman Coulter |
| <b>CD11c</b>    | APC                 | S-HCL-3      | BD              |
| <b>CD14</b>     | Alexa-700           | M5E2         | BD pharmingen   |
| <b>CD69</b>     | V450                | FN50         | BD horizon      |
| <b>CD66</b>     | FITC                | TET2         | Miltenyi        |
| <b>CD123</b>    | PC7                 | 7G3          | BD pharmingen   |
| <b>NKp44</b>    | Pure                | 2.29         | Miltenyi        |

Table SII. Antibodies used in ICS experiments.

| <b>Antibody</b>                | <b>Fluorochrome</b> | <b>Clone</b> | <b>Supplier</b> |
|--------------------------------|---------------------|--------------|-----------------|
| <b>CD3</b>                     | APC-Cy7             | SP34-2       | BD pharmingen   |
| <b>CD45</b>                    | PerCP               | D058-1283    | BD pharmingen   |
| <b>CD8</b>                     | V500                | RPA-T8       | BD pharmingen   |
| <b>CD154</b>                   | FITC                | TRAP1        | BD pharmingen   |
| <b>IL2</b>                     | APC                 | MQ1-17H12    | BD pharmingen   |
| <b>IFN-<math>\gamma</math></b> | V450                | B27          | BD horizon      |
| <b>TNF-<math>\alpha</math></b> | A700                | BMAb11       | BD pharmingen   |
| <b>MIP-1<math>\beta</math></b> | PE                  | D21-1351     | BD pharmingen   |
| <b>CD4</b>                     | PC7                 | L200         | BD pharmingen   |